JOURNAL OF APPLIED PHYSICS **101**, 044511 (2007)

IF impedance and mixer gain of NbN hot electron bolometers

J. W. Kooi[a)]
California Institute of Technology, MS 320-47, Pasadena, California 91125

J. J. A. Baselmans
SRON National Institute for Space Research, Sorbonnelaan 2, 3584 CA Utrecht, The Netherlands

M. Hajenius and J. R. Gao
SRON National Institute for Space Research, Sorbonnelaan 2, 3584 CA Utrecht, The Netherlands and Kavli Institute of Nanoscience, Delft University of Technology, Lorentzweg 1, 2628 CJ Delft, The Netherlands

T. M. Klapwijk
Kavli Institute of Nanoscience, Delft University of Technology, Lorentzweg 1, 2628 CJ Delft, The Netherlands

P. Dieleman, A. Baryshev, and G. de Lange
SRON Netherlands Institute for Space Research, Landleven 12, 9747 AD Groningen, The Netherlands

(Received 4 August 2006; accepted 19 September 2006; published online 27 February 2007)

The intermediate frequency (IF) characteristics, the frequency dependent IF impedance, and the mixer conversion gain of a small area hot electron bolometer (HEB) have been measured and modeled. The device used is a twin slot antenna coupled NbN HEB mixer with a bridge area of $1\times 0.15\ \mu\mathrm{m}^2$, and a critical temperature of 8.3 K. In the experiment the local oscillator frequency was 1.300 THz, and the (IF) 0.05–10 GHz. We find that the measured data can be described in a self-consistent manner with a thin film model presented by Nebosis *et al.* [Proceedings of the Seventh International Symposium on Space Terahertz Technology, Charlottesville, VA, 1996 (unpublished), pp. 601–613], that is based on the two temperature electron-phonon heat balance equations of Perrin-Vanneste [J. Phys. (Paris) **48**, 1311 (1987)]. From these results the thermal time constant, governing the gain bandwidth of HEB mixers, is observed to be a function of the electron-phonon scattering time, phonon escape time, and the electron temperature. From the developed theory the maximum predicted gain bandwidth for a NbN HEB is found to be 5.5–6 GHz. In contrast, the gain bandwidth of the device under discussion was measured to be ~2.3 GHz which, consistent with the outlined theory, is attributed to a somewhat low critical temperature and nonoptimal film thickness (6 nm). © *2007 American Institute of Physics*.
[DOI: 10.1063/1.2400086]

I. INTRODUCTION

Traditionally hot electron bolometer mixers,[1] based on InSb, suffer from small (<100 MHz) IF bandwidths, due to a relatively long electron relaxation time. To enhance the science that may be done with these devices, there has in recent years been a strong push to expand the gain and noise bandwidth of hot electron bolometers. Success has been achieved with the use of ultra thin (≈4–6 nm) NbN superconducting films with very short phonon escape times.[2] The majority of such films have been supplied by the Moscow Pedagogical State University.[3,4] In previous work, measurement and analysis of the IF impedance and gain bandwidth of large area NbN phonon-cooled hot electron bolometers were performed by Rodrigues-Morales and Yngvesson.[5] The analysis was, however, based on model that uses a single time constant to describe the electron temperature relaxation time.[6]

Initially, HEB mixers were analyzed as lumped element transition-edge sensors.[7,8] The strong temperature dependence of the resistance at the transition to the superconducting state was taken as a sensitive measure of variations in the electron temperature. In practice HEB's are operated at an elevated electron temperature created by dc bias and applied local oscillator (LO) signal. These conditions have led to a reanalysis of the physical conditions during mixing. Initially, mixing was understood to be the result of a heating induced, fully normal (Ohmic) electronic "hot spot,"[9] and more recently due to a distributed temperature profile[10,11] in response to temperature and current induced local resistivity. In general, HEB analyses have focused on taking into account all contributions to the power fed into the electron system, balanced by losses due to diffusion and electron-phonon relaxation. In recent work[12] it became clear that the dc current-voltage characteristics could not be described on the basis of power and electron temperatures alone. It turned out important to include the physical process that acts as the source of resistance in a superconducting film close to its transition temperature. This resistance is known to appear due to temperature and current enhanced two-dimensional (2D) phase slip events or flux flow. It was shown[12] that this consider-

[a)]Electronic mail: kooi@submm.caltech.edu; URL: http://www.submm.caltech.edu/cso/receivers.html

ation leads to a correct description of the dc $I(V)$ characteristics. It is assumed that the underlying physics is analogous to the Berezinskii-Kosterlitz-Thouless treatment, in which for thin superconducting films above a characteristic temperature $T > T_{KT}$ pairs of free vortices with plus and minus signs and core radii ξ ($\sim$4 nm for NbN) are created.

In the present manuscript we focus on the dynamic processes that govern the HEB mixer gain, IF impedance, and gain bandwidth. It is assumed that the mixing process at terahertz frequencies is controlled by the quadratic response to voltage, leading to an intermediate frequency signal in the electron temperature. We will assume that the vortex processes relevant at dc are too slow to follow the responses at terahertz and IF frequencies. We find that the two temperature electron cooling model introduced by Perrin-Vanneste,[13] and expanded upon by Nebosis, Semenov, Gousev, and Renk[14] (NSGR) is very adequate in describing the IF response. The NSGR model includes an electrothermal feedback mechanism that modulates mixer's inhomogeneous nonlinear mixing region via complex IF voltage reflections. It is this feedback mechanism that is responsible for fluctuations in the receiver noise temperature.

In this paper we present a unique data set and demonstrate that the modified NSGR model provides a self-consistent set of parameter values in good agreement with literature and measurement. The obtained parameter values may then be used to explore the maximum achievable bandwidth of NbN based HEB's and provide guidance toward possible material improvement.

II. THEORY

At RF frequencies with $h\nu \gg 2\Delta$, power is absorbed uniformly in a bridge with fixed cross-sectional area. Applying a LO signal the electron temperature in the bridge modulates with $[\sin(\omega_{LO}t)+\sin(\omega_s t)]^2$, resulting in a modulation of the electron temperature at the difference frequency (IF) between ω_{LO} and ω_s. Since the upper frequency limit for nonequilibrium responses of the superconductors is set by the superconducting energy gap we assume that the vortex processes cannot follow the RF signals.

At IF's the free vortex density modulation as a result of current is, when compared to the electron temperature, expected to be a lower order effect. In addition, though Knoedler and Voss have measured phase slip induced shot noise up to 100 kHz,[15] the recombination/annihilation rate of free vortices at the intermediate frequencies we concern ourselves with is thought to be too slow to follow the IF signal. We will therefore assume that at the IF's the temporal response is predominantly connected to the electron temperature ($\partial R/\partial T$). This allows the use of the NSGR model, where the nonthermal action of the current ($\partial R/\partial I$) has been neglected.

The primary cooling mechanism of quasiparticles in the superconducting film occurs via electron-phonon interaction, while the phonons, raised to a temperature that closely follows the electron temperature, escape into the substrate. Due to the thin (3.5–6 nm) film and strong coupling to the substrate, diffusion via the metal contact pads is assumed negligible in determining the temporal response. For this reason diffusion has been neglected in the NSGR model. Important to our discussion are the strongly temperature dependent heat capacities of the electrons, $c_e(T_e)$, and phonons, $c_{ph}(T_{ph})$. Following the two temperature analyses of Perrin-Vanneste,[13] coupled differential equations are used, one for the electron temperature T_e and one for the phonon temperature T_{ph}, to describe the heat balance in the film:

$$c_e \frac{\partial T_e}{\partial t} = P_{dc} + p_{LO} - p_{eph}, \tag{1}$$

$$c_{ph} \frac{\partial T_{ph}}{\partial t} = p_{eph} - p_{phs}. \tag{2}$$

The powers are per unit volume, with P_{dc} and p_{LO} due to dc and LO power induced heating. p_{eph} describes the power transfer between the quasiparticles and the phonons, and p_{phs} the transfer between phonons and substrate (with a bath temperature T_0).

$$p_{eph} = A_e(T_e^n - T_{ph}^n), \quad A_e = \frac{c_e}{nT_e^{n-1}\tau_{eph}}, \tag{3}$$

$$p_{phs} = A_{ph}(T_{ph}^4 - T_0^4), \quad A_{ph} = \frac{c_{ph}}{nT_{ph}^3\tau_{esc}}. \tag{4}$$

For NbN, $n \sim 3.6$.[16,17] Both p_{eph} and p_{phs} are assumed uniform in the bridge apart from their temperature dependence.[14,18] In reality, the temperature profile across the bridge is a function of position,[11,12] and even though this has not been taken into account in the NSGR model, we are able to achieve good fits between model and measurement. Future models may be improved by taking the distributed temperature profile across the bridge into account.

To obtain a general solution to the heat balance equations, one has to make a certain assumption on how the local resistivity depends on current and electron temperature. Following Nebosis *et al.*, we obtain

$$Z = \frac{d}{dI}[IR(I,T_e)] = R(I,T_e) + I\frac{\partial R}{\partial I} + I\frac{\partial R}{\partial T_e}\frac{\partial T_e}{\partial I}, \tag{5}$$

where term $\partial R/\partial I$ is ignored at IF's. $Z(\omega)$, the frequency dependent HEB output impedance, may be found by assuming that a small perturbation in the current, $dI = \delta I e^{i\omega t}$, causes a change in the electron temperature, $dT_e = \delta T_e e^{i(\omega t+\varphi 1)}$, and phonon temperature $dT_{ph} = \delta T_{ph} e^{i(\omega t+\varphi 2)}$. Substituting these partials into the linearized ($T_e \sim T_{ph} \ll 2T_0$) heat balance, Eqs. (1) and (2), and solving it together with Eq. (5) give

$$Z(\omega) = R_o \frac{\Psi(\omega)+C}{\Psi(\omega)-C}. \tag{6}$$

Strictly speaking the simplification that $T_e \sim T_{ph}$ holds (Sec. VI), however, the assumption that $T_{ph} \ll 2T_0$ and that of a uniform temperature distribution in the bridge is not entirely valid as it approximates a lumped element model. It does, however, provide a convenient closed form solution that fits the measured data. In Eq. (6), $\Psi(\omega)$ represents the time dependent modulation of the electron temperature, ω the IF radial frequency, R_o the dc resistance at the operating point

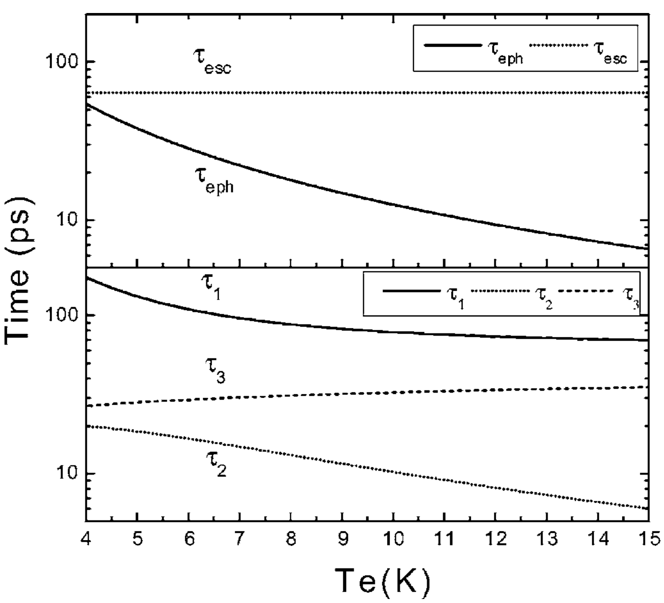

FIG. 1. Discussed time constants and their electron temperature relationship. The NbN τ_{eph}, τ_{esc}, and the heat capacity ratio c_e/c_{ph} (not shown) are obtained from literature and serve to constrain the impedance and mixer gain models. A 6 nm thick NbN film is estimated from transmission electron microscopy (TEM) measurements, with values for τ_1, τ_2, τ_3 derived from Eqs. (9)–(11). Actual fit values for τ_{eph}, τ_{esc}, and c_e/c_{ph} for different HEB bias and LO pump conditions are shown in Table I.

of the mixer, and C the self heating parameter.[19,20] The latter is important as it forces the complex part of the impedance [Eq. (6)] to be zero at very low and very high IF frequencies. $\Psi(\omega)$ is defined by three time constants, τ_1, τ_2, τ_3:

$$\Psi(\omega) = \frac{(1+i\omega\tau_1)(1+i\omega\tau_2)}{(1+i\omega\tau_3)}. \tag{7}$$

The self-heating parameter C can be described as

$$C = \frac{I^2}{V}\frac{\partial R}{\partial T_{\mathrm{e}}}\left(\frac{\tau_{\mathrm{eph}}}{c_{\mathrm{e}}} + \frac{\tau_{\mathrm{esc}}}{c_{\mathrm{ph}}}\right), \tag{8}$$

with dV/dI the differential resistance at the operating point. In the transfer function $\Psi(\omega)$, τ_1, τ_2, τ_3 may be solved as

$$\tau_1^{-1}, \tau_2^{-1} = \frac{\Omega}{2}\left(1 \mp \sqrt{1 - \frac{4\tau_{\mathrm{eph}}^{-1}\tau_{\mathrm{esc}}^{-1}}{\Omega^2}}\right), \tag{9}$$

with

$$\Omega = \left(1 + \frac{c_{\mathrm{e}}}{c_{\mathrm{ph}}}\right)\tau_{\mathrm{eph}}^{-1} + \tau_{\mathrm{esc}}^{-1}, \tag{10}$$

and

$$\tau_3^{-1} = \frac{c_{\mathrm{e}}}{c_{\mathrm{ph}}}\tau_{\mathrm{eph}}^{-1} + \tau_{\mathrm{esc}}^{-1}. \tag{11}$$

In Fig. 1 we plot the phonon escape time and electron-phonon scattering time with the corresponding $\Psi(\omega)$ time constants as a function of electron temperature for a 6 nm NbN superconducting film.

To derive an expression for the conversion gain of the mixer, we use standard lumped element formalism to obtain the frequency selective responsivity[8,21,22] of a bolometer, but with the single pole time constant replaced by the more general temperature dependent electron transfer function $\Psi(\omega)$. Included in the responsivity is a complex load impedance Z_l, which connects across the output port of the bolometer, and the HEB output reflection coefficient Γ_{IF} In this manner the self-heating electrothermal feedback, due to (complex) voltage reflections between mixer and IF circuitry, may be taken into account.

$$S(\omega) = \frac{dV_l}{dP} = \frac{\alpha}{\chi I}\frac{Z_l}{R_o + Z_l}\frac{C}{[\Psi(\omega) + \Gamma_{\mathrm{IF}}C]}, \tag{12}$$

with

$$\Gamma_{\mathrm{IF}} = \frac{R_o - Z_l}{R_o + Z_l}. \tag{13}$$

Here α represents the RF coupling factor, and I the signal current thruough the load (and device). Fundamentally the bolometer responsivity of Eq. (12) remains linked to the lumped element model, and a modification is needed to properly account for the different heating efficiencies of LO and dc signal power.[10] This parameter is symbolized by χ and is an inverse measure of the width of the distributed temperature profile in the bridge. At high bias power $\chi \sim 1$, whereas at low dc bias and incident LO power χ may be as large as 3. Obtained values for χ in the context of the present analyses are found in Table II. In this formalism, the direct detection (bolometric) response of the hot electron bolometer[23] may be accounted for by a change in χ, bias current, and R_o. Regardless of these adjustments, the modified NSGR hot electron bolometer responsivity remains an approximation of the physical dynamics inside the bridge area,[12] albeit a good one.

Note that because the IF load impedance connected to the mixer is in general complex, it is important to use the complex responsivity, and not the absolute responsivity, $|S(\omega)|$, to reflect the true nature of the electrothermal feedback on the conversion gain, $\eta(\omega)$. To find the (complex) conversion gain of the mixer, we use the standard expression

$$\eta(\omega) = \frac{2S(\omega)^2}{Z_l}p_{\mathrm{LO}}. \tag{14}$$

After substitution of Eq. (12), and making the assumption that most of the signal current through the device is, in fact, dc bias current, i.e., $P_{\mathrm{dc}}=I^2R_o$ we find after some algebraic manipulation the magnitude of the conversion gain as

$$\eta(\omega) = \frac{2\alpha^2 p_{\mathrm{LO}}}{\chi^2 P_{\mathrm{dc}}}\left|\frac{R_o Z_l}{(R_o+Z_L)^2}\frac{C^2}{[\Psi(\omega)+\Gamma_{\mathrm{IF}}C]^2}\right|, \tag{15}$$

where p_{lo} is the LO power at the device, as estimated from the isothermal technique.[24,25]

III. EXPERIMENT AND CALIBRATION

In the described experiment we use a submicron twin-slot NbN HEB mixer chip (M12-F2) with a bridge area of 1×0.15 μm.[2] Before processing the starting film had a T_c of 9.5 K. After fabrication the critical temperature of the submicron area HEB lowered to 8.3 K. Details on device's noise temperature, mixer gain as a function of bias, and R-T curve may be found in a separate paper by Yang *et al.*[26] To obtain the 1.3 THz (Ref. 27) LO pumped HEB IF impedance the

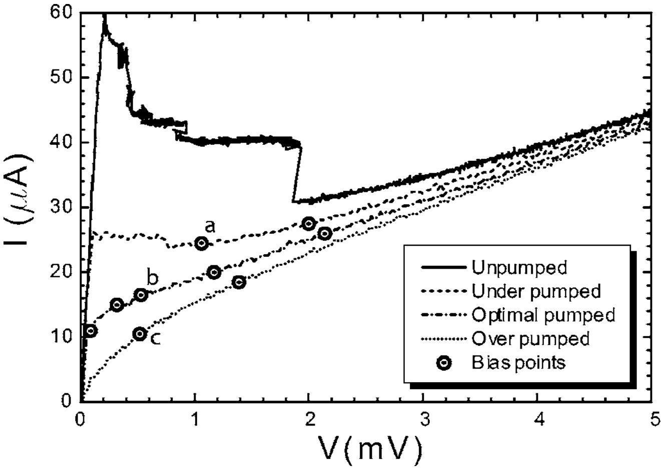

FIG. 2. Unpumped, underpumped, optimal pumped, and over pumped I/V curves. Circles indicate the bias points where reflection and mixer gain measurements were obtained. a, b, and c refer to the impedances shown in Fig. 3.

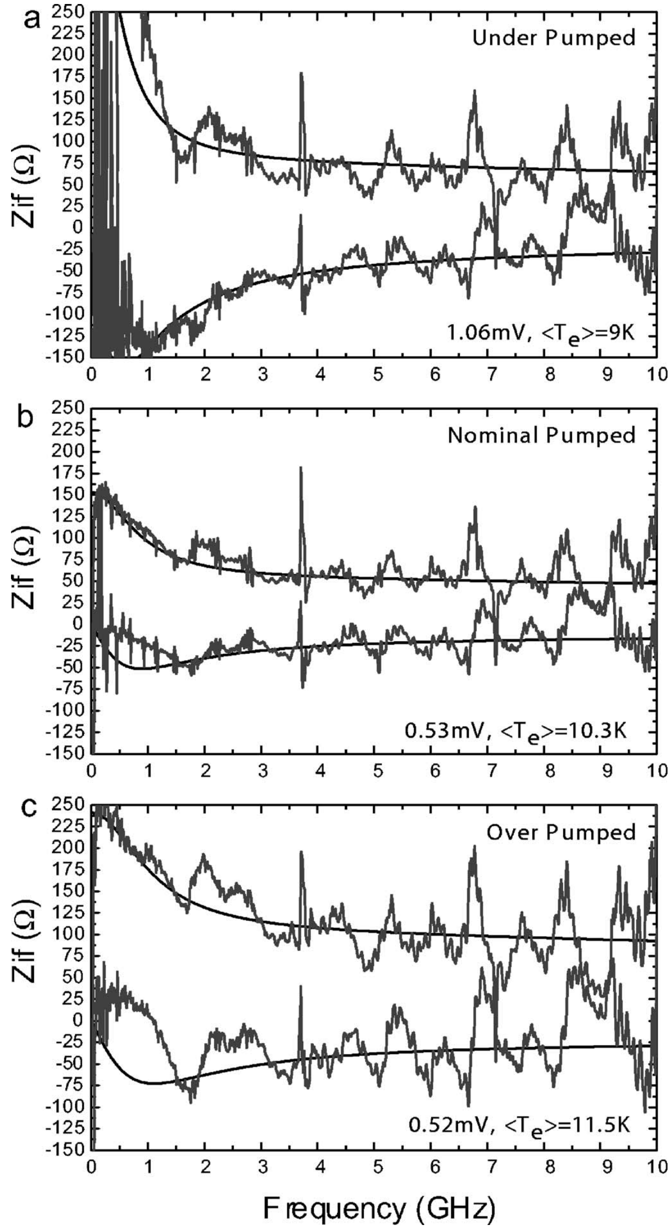

FIG. 3. Measured and modeled IF impedance for a variety of bias and LO pump power conditions. The mean electron temperature is a fit parameter in the model and is found, consistent with theory, to increase with the LO pump level. Refer to Fig. 4 for related mixer gain and Tables I and II for additional details.

following procedure was used: At 4.2 K we measured the complex reflection coefficient of the mixer block IF output with a vector network analyzer (VNA). The output power of the VNA was −65 dBm, low enough not to disturb the HEB I/V curve. To improve the signal to noise ratio, 64 measurements were averaged. Included in the VNA measurement is a bias tee. Next we used HFSS,[28] a full three-dimensional (3D) finite element electromagnetic field simulator, to obtain a two port S-parameter model of the mixer block IF circuit, including wire bonds, via holes, and air space. Finally, to obtain the actual LO pumped HEB IF impedance, a linear circuit simulator[29] was employed to deembed the IF circuit from the VNA measurement. Further details on the calibration method may be found at Ref. 30. Though not applied here, it is also possible to eliminate the need of a full deembedding of the HEB mixer IF circuitry by using the mixer itself as a calibration source. This can be achieved with the HEB inside the cryostat. Here we use the HEB in its superconducting state as a short, and the HEB at 20 K as a load with known impedance. Measuring the full S11 reflection coefficient at both states enables a full calibration of the VNA, with the reference plane at the HEB bridge itself. This technique eliminates the need of a 3D electromagnetic simulation, facilitating experimental analyses.

IV. IF IMPEDANCE

In Fig. 2 we show the bias points at which reflection and mixer gain measurements in the experiment were obtained. The bias points are chosen strategically along three (over-, optimal-, and underpumped) LO levels. The measured HEB IF impedance and mixer conversion were fitted against the model using Eqs. (6)–(11) to determine the IF impedance, and Eq. (16) to obtain the mixer gain (Sec. V). It was found essential to use both the measured impedance and calibrated mixer gain data to obtain a self-consistent fit for τ_{eph}, τ_{esc}, and the temperature dependent $c_{\mathrm{e}}/c_{\mathrm{ph}}$ ratio.

Figure 3 represents a subset of the data presented in Ref. 30. We find that particularly in the underpumped LO situation, the HEB IF impedance demonstrates large real and reactive components. It is here that the mean electron temperature is lowest. For all bias conditions[30] in the range of 0–3 GHz, where the mixer gain is optimal, the real and imaginary components of the IF impedance are most dynamic, and a proper match to 50 Ω is difficult. The reason for this behavior is that the effect of τ_1 and τ_3 in the time dependent electron temperature, $\Psi(\omega)$, is largest in this frequency range (see also Fig. 5). The electrothermal feedback, via voltage reflections of the HEB superconducting bridge, is therefore most pronounced in the IF region with optimal mixer gain.

The input parameters for the fit procedure and resulting values for the fit parameters are shown in Table I. These parameters provide interesting statistics on the material prop-

TABLE I. HEB parameters for different bias conditions. Units of dV/dI, R_o, R_o^* are in Ω, $\tau_{\rm esc}$, and $\tau_{\rm eph}$ in ps, $T_{\rm e}$(eph), and $T_{\rm e}(c_{\rm e}/c_{\rm ph})$ in Kelvin. Each row has three data sets ($Z_{\rm re}$, $Z_{\rm im}$, $G_{\rm mix}$) which are used to obtain a self-consistent set of fit values. The first three columns (dV/dI, R_o, and C) are derived from the measured I/V curve. The three primary fit parameters are $\tau_{\rm esc}$, $\tau_{\rm eph}$, and $c_{\rm e}/c_{\rm ph}$. These determine the electron temperature time dependence. For some bias and LO settings it was found that the dc resistance at the operating point (R_o) and self heating parameter (C) needed adjustment. The modified values are depicted by R_o^* and C^*. Especially in the more extreme bias states did we find significant changes to R_o and C. This is likely due to the lumped element nature of the NSGR model, which does not completely account for all the dynamics inside the bridge area (Ref. 12). $T_{\rm e}$(eph) and $T_{\rm e}(c_{\rm e}/c_{\rm ph})$ are mean electron temperatures inferred from fit values of $\tau_{\rm eph}$ and $c_{\rm e}/c_{\rm ph}$, and the obtained temperature relationships from literature (Refs. 22, 31, and 32).

V bias	dV/dI	R_o	C	R_o^*	C^*	$\tau_{\rm esc}$	$\tau_{\rm eph}$	$c_{\rm e}/c_{\rm ph}$	$T_{\rm e}$(eph)	$T_{\rm e}(c_{\rm e}/c_{\rm ph})$
0.09 mV opt	42	7.5	0.69	10.0	0.55	45.8	15.8	0.24	8.6	8.9
0.32 mV opt	110	21.3	0.67	27.5	0.62	65.4	12.7	0.22	9.9	9.3
0.53 mV opt	167	31.2	0.68	37.0	0.61	72.0	12.3	0.18	10.2	10.3
1.17 mV opt	168	58.5	0.48	58.5	0.48	65.8	10.3	0.15	11.3	11.4
2.14 mV opt	169	82.3	0.34	82.3	0.34	58.4	7.3	0.10	13.9	13.7
20.0 mV opt	150	140	0.034	40	0.033	⋯	⋯	⋯	⋯	⋯
1.06 mV under	600	42.4	0.87	52.4	0.77	65.2	14.9	0.24	9.0	8.9
2.00 mV under	230	71.4	0.53	66.0	0.33	68.2	9.1	0.13	12.2	12.3
0.52 mV over	80	52.0	0.21	70.0	0.55	70.2	10.0	0.15	11.5	11.4
1.39 mV over	127	77.2	0.24	50.0	0.24	65.4	7.7	0.11	13.5	13.4

erties of the NbN film, and assumptions of the temperature dependence of $\tau_{\rm eph}$, and $c_{\rm e}/c_{\rm ph}$ used in literature. For example, the mean escape time for phonon's into the substrate is 64±4.9 ps. Using the empirical relationship that $\langle\tau_{\rm esc}\rangle \approx 10.5d$ (ps/nm),[31,32] we find a suggestive NbN film thickness of 6.1±0.46 nm. This is supported by a recent study of the film by transmission electron microscopy (TEM), in which the measured thickness is 6±1 nm instead of the intended 3.5 nm thickness.[33] In addition, the temperature relationship of the electron-phonon interaction time, and the ratio of the electron-phonon heat capacities may, to a first order, be verified. Using the empirical relationships that for thin NbN films, $\tau_{\rm eph} \approx 500T^{-1.6}$ (ps K) (Ref. 22) and $c_{\rm e}/c_{\rm ph} \approx 18.77T^{-2}$,[32] we obtain an estimate for the mean (or effective) electron temperature in the NbN bridge. The last two columns in Table I show the calculated results. The mean electron temperature, $\langle T_{\rm e}\rangle = \langle T_{\rm e}({\rm eph}) + T_{\rm e}(c_{\rm e}/c_{\rm ph})\rangle$, is reported in Fig. 3 and shows a consistent trend with bias and LO pump level.[10,11]

V. MIXER CONVERSION GAIN AND THE EFFECT OF ELECTROTHERMAL FEEDBACK

To properly model the HEB mixer conversion gain, the effect of voltage reflections on the electron temperature and subsequent mixing efficiency ($\partial R/\partial T$) will need to be taken into account. This is important as voltage reflections at the IF port cause, via a self-heating electrothermal feedback mechanism, fluctuations in the mixer gain.

From experience it is known that there are some discrepancies between measurement and theory with existing HEB mixer models. One of these is due to an oversimplification of the IF impedance presented to the hot electron bolometer mixer.[4,5,8,10,14] In nearly all instances, the IF impedance used in the electrothermal feedback formulism is assumed real. In actuality the IF impedance presented to the active device is both complex and frequency dependent. Because, as part of the deembedding exercise, an accurate 3D EM model[28] of the IF embedding circuit inclusive of discontinuities and wire bonds was developed, it can now also be used to accurately predict the IF impedance presented to the HEB mixer chip. With this information we are able to calculate $\Gamma_{\rm IF}$ and $[R_oZ_l/(R_o+Z_l)^2]$ in Eq. (15). A second problem with the traditional (idealized) mixer gain calculations is that it does not include a mechanism to account for parasitic device reactance. These can, for example, be introduced in the HEB mixer stripline circuitry, contact pads, and capacitance across the bridge. It is, however, also possible that it is related to an incomplete model of the HEB mixer. Since parasitic device reactance is not taken into account in the "idealized" responsivity formulism of Eq. (12), it may be advisable to include them. We find experimentally that the addition of a 10 GHz (τ=15.8 ps) fixed frequency pole to Eq. (15) helps to improve the high frequency accuracy of the modeled conversion gain. At low IF's where the vast majority, if not all, of HEB's operate the addition of an added pole to $\eta(\omega)$ and $Z(\omega)$ is of little consequence.

A final issue that needs addressing is the need for an efficiency factor. It is known, for example, that the hot electron bolometer mixer conversion gain and LO pumped I/V curves are RF dependent. This is understood to be due to the heating efficiency of the "hot" electrons and the distributed temperature profile in the bridge (χ, Sec. II). The HEB mixer gain modified for device parasitics and heating efficiency may thus be rewritten as

$$\eta(\omega) = \frac{2\alpha^2 p_{\rm LO}}{\chi^2 P_{\rm dc}} \left| \frac{1}{(1+i\omega\tau_p)^2} \frac{R_o Z_l}{(R_o+Z_L)^2} \frac{C^2}{[\Psi(\omega)+\Gamma_{\rm IF}C]^2} \right|, \tag{16}$$

where $\tau_p \approx 15.8$ ps. Note that τ_p is device and application dependent. α, the optical coupling factor, is estimated to be 0.66 (−1.8 dB). In Fig. 4 we show the measured and modeled mixer gain for three different biases and LO pump conditions. Fit parameters for the entire data set are shown in Tables I and II. Based on these results, Eq. (16) is seen to accurately describe both the amplitude and frequency dependence of the HEB mixer conversion gain.

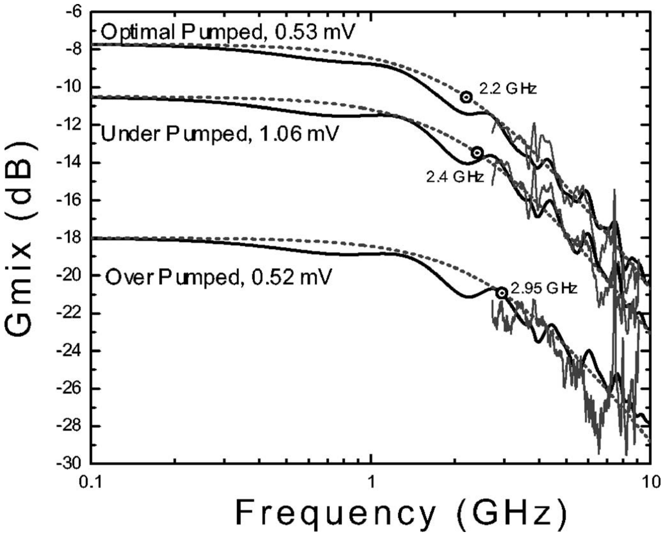

FIG. 4. Measured and modeled HEB mixer conversion gain as a function of IF frequency for the three bias conditions in Fig. 3. The −3 dB gain rolloff shifts to higher frequency with increased LO power. This is understood to be caused by the increased mean electron temperature. The effect of electro-thermal feedback is taken into account by means of the (modeled) complex IF load impedance. Details in Tables I and II.

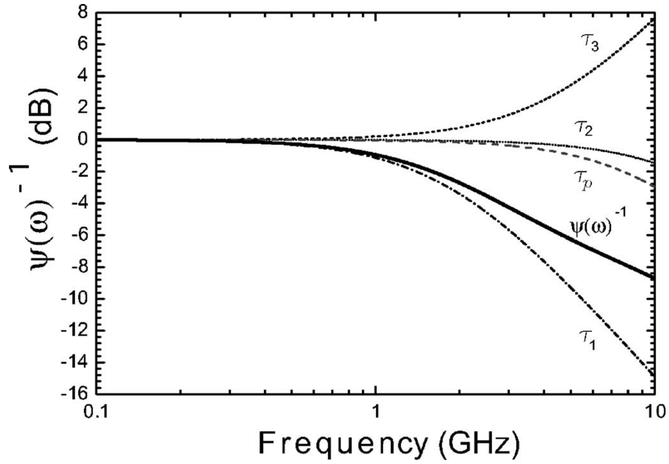

FIG. 5. $\Psi(\omega)^{-1}$ (dB), the time dependent transfer function of the electron temperature at 0.53 mV bias and optimal LO pump level. $\tau_1=87.1$ ps, which results in a pole at 1.83 GHz. $\tau_2=10.1$ ps with a pole at 15.8 GHz, and $\tau_3=35.0$ ps with a zero at 4.55 GHz. Also shown is τ_p which accounts for device parasitics. The poles and zero effectively synthesize a "single" 2.20 GHz pole. To increase the IF bandwidth, the time response of $\Psi(\omega)$ will need to be increased.

Some observations can be made: First, to minimize receiver noise temperature modulation across the IF operating bandwidth, one has to carefully consider ways to minimize the complex part of Z_l at the superconducting bridge such that Γ_{IF} is frequency independent. Second, setting $Z_l \approx R_o$ such that $\Gamma_{\mathrm{IF}} \rightarrow 0$ not only minimizes the frequency dependent modulation of $\eta(\omega)$ but also maximizes the mixer gain. To do so in practice, it is desirable to terminate the reflected noise wave by means of a balanced amplifier or isolator between the mixer unit and the first low noise amplifier. It also requires a good understanding of the IF circuit (matching network and bias tee) including wire bonds that connect the HEB mixer chip.

To better understand how the time dependent electron transfer function and the parasitic device capacitance determine the HEB gain bandwidth and overall slope, we plot in Fig. 5 $\Psi(\omega)^{-1}$, and the transfer functions $(1+i\omega\tau_1)^{-1}$, $(1+i\omega\tau_2)^{-1}$, $(1+i\omega\tau_3)$, and $(1+i\omega\tau_p)^{-1}$ at 0.53 mV bias and optimal LO signal level. Here τ_3 (4.55 GHz) is seen to slightly compensate τ_1 (1.83 GHz), whereas τ_2 (15.8 GHz) enhances the effect of τ_1, though to a very small extent. Adding τ_p to take into account residual device parasitics, we effectively synthesize a 2.20 GHz pole in $\eta(\omega)$ as indicated in Eq. (16). This is also depicted by ν_{NSGR} in Table II. As may be seen from Table II, the IF bandwidth is bias and LO power dependent. By biasing the HEB mixer at a higher bias voltage (electron temperature), IF bandwidth and conversion efficiency may to some extent be traded off. This effect is in good agreement with results from literature.[4,6,34,35]

VI. INCREASING THE IF BANDWIDTH OF HOT ELECTRON BOLOMETERS

For many radio-astronomy and atmospheric science applications the 2–3 GHz IF bandwidth reported here would be too small. Since $\Psi(\omega)^{-2} \propto \eta(\omega)$, it is meaningful to study the time dependent electron temperature to gain insight into ways in which the HEB mixer IF bandwidth may be enhanced. A close inspection of Eqs. (10) and (11), as shown in Fig. 6, indicates that a rise in the electron and phonon temperature results in a faster response time and therefore an improved gain bandwidth. The physical explanation is that with increasing temperature the phonon specific heat (c_{ph}) increases faster than the electron specific heat (c_e). Phonons are thus seen to act as an important intermediate heat bath between the electron gas and substrate. Note that for thinner films this effect is enhanced. Because thin films of NbN can have different critical temperatures depending on deposition conditions and thickness, it is important that both the critical temperature and thickness of the film be optimized. As a corollary, use of higher T_c materials with strong electron-phonon interaction and a short phonon escape time should also be of benefit. Thus by reducing the film thickness one can increase the IF bandwidth, while for a given thickness an increased T_c will also result in an increased bandwidth (Fig. 6).

TABLE II. Mixer gain parameters. ν_{NSGR} is the modeled −3 dB gain bandwidth (GHz), and ν_{expt} the experimentally obtained −3 dB gain bandwidth. χ describes the ratio of LO power to dc power heating efficiency. p_{LO} in nW, and the LO frequency 1.3 THz (Ref. 27).

Vbias	χ	ν_{NSGR}	ν_{expt}	p_{LO}
0.09 mV opt	2.632	2.10	1.8	55
0.32 mV opt	1.632	1.95	2.0	55
0.53 mV opt	1.365	2.20	2.3	55
1.17 mV opt	1.118	3.00	3.2	55
2.14 mV opt	0.978	3.80	4.0	55
20.0 mV opt	⋯	⋯	⋯	⋯
1.06 mV under	1.114	2.40	2.4	29
2.00 mV under	0.854	3.15	3.4	29
0.52 mV over	2.623	2.95	3.0	72
1.39 mV over	1.379	3.00	3.3	72

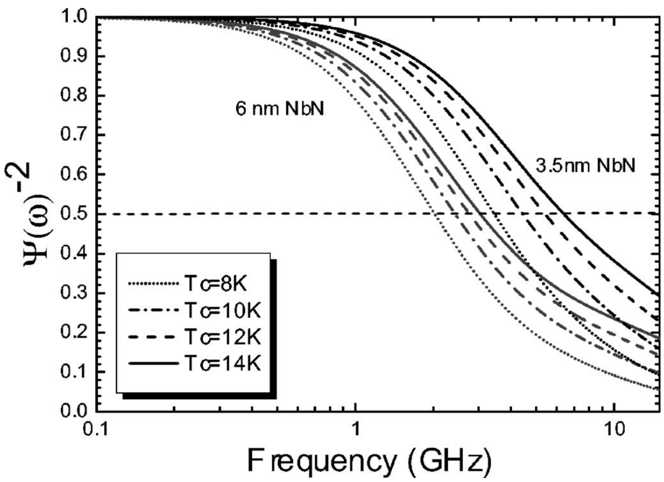

FIG. 6. $\Psi(\omega)^{-2}$ as a function of IF frequency for 3.5 and 6 nm thickness NbN films of different T_c. $\Psi(\omega)^{-2}$ can be interpreted as the relative conversion gain without the effect of electrothermal feedback. For an optimized NbN mixer the maximum gain bandwidth is projected to be on the order of 5.5–6 GHz.

The temperature dependence in Fig. 6 is derived under the assumption that $T_e \sim T_{ph}$. To estimate the difference between T_e and T_{ph} for actual operating conditions, T_e and T_{ph} were calculated, using Eqs. (1) and (2). Under these conditions T_{ph} is approximately $0.8T_e$, which in view of the small difference suggests that the Perrin-Vanneste two temperature model is applicable to the hot electron bolometers under discussion. In the case of the homogeneous model, the T_c of the film is thus found to be a measure of the electron temperature. However, there is a distributed temperature profile[10–12] in HEB mixers, which inevitably leads to deviations from the uniform temperature calculations of Perrin-Vanneste. The temperature in the center of the HEB bridge, depending on, for example, the interface transparency of the contacts and the operating condition, can in general exceed the critical temperature of the film (Table I). It may therefore be argued that the IF bandwidth follows the T_c dependence as shown in Fig. 6, with possibly an enhanced bandwidth as a result of higher electron temperature due to device size, interface contact transparency, high bias, or overpumped LO. The by the co-authors reported IF bandwidth measurement of 6 GHz (Ref. 34) was performed on a much larger area device ($4 \times 0.4\ \mu m^2$), with clean contacts that is not necessarily the same as the device under discussion. Although not fully understood, the result remains within the theoretical possibility of the presented analyses.

VII. CONCLUSION

A deembedding technique is demonstrated to obtain the IF impedance of a small area ($0.15\ \mu m^2$) phonon-cooled HEB under a variety of bias and LO pump level conditions. In the same setup the HEB mixer conversion gain has, at an LO frequency of 1.3 THz, been measured in a 2.5–9 GHz IF bandwidth.

To understand the observations, we have successfully modeled the HEB IF impedance and mixer conversion gain based on a two temperature electron cooling model by Perrin-Vanneste and expanded upon by Nebosis *et al.* Good agreement in both amplitude and frequency between model and theory is obtained, and we are able to extract from the NSGR model values for the electron-phonon interaction time τ_{eph}, the phonon escape time τ_{esc}, and the ratio of the electron and phonon specific heat capacity c_e/c_{ph}. Indirectly, using published temperature and thickness relationships for NbN, we are able to infer the effective electron temperature of the bridge as a function of bias, LO pump level, and the thickness of the NbN film (6 nm for the device in this experiment). As the electron temperature of the bridge varies, the electron transfer time changes, influencing the IF impedance and mixer gain bandwidth. Because the phonon and electron heat capacity ratio for NbN is a strong function of temperature, it is found that along with a reduction in film thickness it is also important to maximize the critical temperature of the film. Using the NSGR model we are able to infer a maximum achievable IF bandwidth of NbN film HEB's of ~5.5–6 GHz.

Finally, by using the complex IF impedance presented to the HEB chip we are able to demonstrate the effect of electrothermal feedback on the mixer gain. Flat mixer gain (receiver noise temperature) within IF band may only be achieved if the variance of the complex load impedance presented to the HEB mixing chip is small compared to the hot electron bolometer dc resistance at its operating point. Mixer gain is maximized when both the load impedances presented to the HEB device is real, close to the dc resistance of the device, and the power exchange function χ close to unity. Thus, using the modified NSGR model with a knowledge of the IF load impedance presented to the HEB mixer and a measured (LO pumped) I/V curve, expressions for the impedance and mixer gain of thin NbN films may now be derived.

ACKNOWLEDGMENTS

The authors thank Willem Jellema, Ronald Hesper, Wolfgang Wild, Thijs de Graauw, and Tom Phillips for their support. They would also like to thank Youjin Deng at Theoretical Physics Group at Delft for checking the mathematical solutions of the time dependent heat balance equations. This work was supported in part by NSF Grant No. AST-0229008 and Radionet.

[1]T. G. Phillips and K. B. Jefferts, Rev. Sci. Instrum. **44**, 1009 (1973).
[2]S. Cherednichenko, P. Yagoubov, K. Il'in, G. Gol'tsman, and E. Gershenzon, *Proceedings of the Eighth International Symposium on Space Terahertz Technology*, Cambridge, MA, 1997 (unpublished), p. 245.
[3]P. Yagoubov, G. Gol'tsman, B. Voronov, L. Seidman, V. Siomash, S. Cherednichenko, and E. Gershenzon, *Proceedings of the Seventh International Symposium on Space Terahertz Technology*, Charlottesville, VA, 1996 (unpublished), pp. 290–302.
[4]H. Ekström, E. Kollberg, P. Yagoubov, G. Gol'tsman, and E. Gerhenzon, Appl. Phys. Lett. **70**, 3296 (1997).
[5]F. Rodrigues-Morales and K. S. Yngvesson, *Proceedings of the 14th International Symposium on Space Terahertz Technology*, Tuscon, AZ, 2003 (unpublished).
[6]B. Karasik and W. McGrath, Int. J. Infrared Millim. Waves **20**, 21 (1999).
[7]D. E. Prober, Appl. Phys. Lett. **62**, 2119 (1993).
[8]B. S. Karasik and I. Elant'ev, Appl. Phys. Lett. **68**, 853 (1996).
[9]D. W. Floet, E. Miedema, T. M. Klapwijk, and J. R. Gao, Appl. Phys. Lett. **74**, 433 (1999).
[10]H. F. Merkel, P. Khosropanah, D. W. Floet, P. A. Yagoubov, and E. L. Kollberg, IEEE Trans. Microwave Theory Tech. **48**, 690 (2000).

[11]T. M. Klapwijk, R. Barends, J. R. Gao, M. Hajenius, and J. J. A. Baselmans, Proc. SPIE **5498**, 129 (2004).
[12]R. Barends, M. Hajenius, J. R. Gao, and T. M. Klapwijk, Appl. Phys. Lett. **87**, 263506 (2005).
[13]N. Perrin and C. Vanneste, J. Phys. (Paris) **48**, 1311 (1987)
[14]R. S. Nebosis, A. D. Semenov, Yu. P. Gousev, and K. F. Renk, *Proceedings of the Seventh International Symposium on Space Terahertz Technology*, Charlottesville, VA, 1996 (upublished), pp. 601–613.
[15]C. M. Knoedler and R. F. Voss, Phys. Rev. B **26**, 449 (1982).
[16]E. M. Gershenson, G. N. Gol'tsman, I. G. Gogidze, Yu. P. Gousev, A. I. Elant'ev, B. S. Karasik, and A. D. Semenov, Sverhprovodimost' (KIAE) **3**, 2143 (1990) [Sov. Phys. Superconductivity **3**, 1582 (1990)].
[17]B. S. Karasik and A. I. Elant'ev, *Proceedings of the Sixth International Symposium on Space Terahertz Technology*, Caltech, Pasadena, CA, 1995 (unpublished), p. 229.
[18]E. M. Gershenson, G. N. Gol'tsman, A. I. Elant'ev, B. S. Karasik, and S. E. Potoskuev, Sov. J. Low Temp. Phys. **14**, 414 (1988).
[19]H. Ekström, B. Karasik, E. Kollberg, and K. Yngvesson, IEEE Trans. Microwave Theory Tech. **43**, 938 (1995).
[20]P. J. Burke, R. J. Schoelkopf, and D. E. Prober, J. Appl. Phys. **85**, 1664 (1999).
[21]D. F. Fillipovic, S. S. Gearhart, and G. M. Rebeiz, IEEE Trans. Microwave Theory Tech. **41**, 1738 (1993).
[22]Yu. P. Gousev, G. N. Gol'tsman, A. D. Semenov, E. M. Gershenzon, R. S. Nebosis, M. A. Heusinger, and K. F. Renk, J. Appl. Phys. **75**, 3695 (1994).
[23]J. J. A. Baselmans *et al.*, Appl. Phys. Lett. **86**, 163503 (2005).
[24]M. Hajenius, J. J. A. Baselmans, A. Baryshev, J. R. Gao, T. M. Klapwijk, J. W. Kooi, W. Jellema, and Z. Q. Yang, J. Appl. Phys. **100**, 074507 (2006).
[25]In Ref. 24 it was found that the isothermal technique is an adequate method of estimating the LO power needed to pump a HEB mixer. It was also found that designing an optical coupling scheme that is capable of matching the highly divergent beam from the silicon lens antenna with more than 50% of efficiency is challenging.
[26]Z. Q. Yang, M. Hajenius, J. J. A. Baselmans, J. R. Gao, B. Voronov, and G. Gol'tsman, Supercond. Sci. Technol. **19**, L9 (2006).
[27]Virginia Diodes, Inc., Charlottesville, VA 22902–6172.
[28]Ansoft Corporation, Pittsburgh, PA 15219.
[29]Microwave Office, Applied Wave Research Inc., El Segundo, CA 90245.
[30]J. W. Kooi *et al.*, *Proceedings of the 16th International Symposium on Space Terahertz Technology*, Goteborg, Sweden, 2–4 May 2005 (unpublished), pp. 465–473.
[31]S. B. Kaplan, J. Low Temp. Phys. **37**, 343 (1979).
[32]A. D. Semenov, R. S. Nebosis, Yu. P. Gousev, M. A. Heusinger, and K. F. Renk, Phys. Rev. B **52**, 581 (1995).
[33]J. R. Gao, M. Hajenius, F. D. Tichelaar, B. Voronov, E. Grishina, T. M. Klapwijk, G. Gol'tsman, and C. A. Zorman, *Proceedings of the 17th International Symposium on Space Terahertz Technology*, Paris, France, 2006 (unpublished).
[34]J. J. A. Baselmans, M. Hajenius, J. R. Gao, T. M. Klapwijk, P. A. J. de Korte, B. Voronov, G. Gol'tsman, Appl. Phys. Lett. **84**, 1958 (2004).
[35]K. V. Smirnov, Yu. B. Vachtomin, S. V. Antipov, S. N. Masalennikov, N. S. Kaurova, V. N. Drakinsky, B. M. Voronov, and G. N. Gol'tsman, *Proceedings of the 14th International Symposium on Space Terahertz Technology*, Tucson, AZ, 2003 (unpublished), pp. 405–409.